Synthesis, Crystal Structure, and Stability of Pyruvoylpentacarbonylmanganese(I)

Charles P. Casey,* Charles A. Bunnell, and Joseph C. Calabrese

Contribution from the Department of Chemistry, University of Wisconsin, Madison, Wisconsin 53706. *Received June 4, 1975*

Abstract: Sodium pentacarbonylmanganese reacts with pyruvoyl chloride to give pyruvoylpentacarbonylmanganese(I) (**4a**), which was characterized by spectral means and by x-ray crystallography. **4a** reacts with 4-ethyl-2,6,7-trioxa-1-phosphabicyclo[2.2.2]octane, ETPO, in a first-order reaction to give $CH_3COCOMn(CO)_4(ETPO)$ (**4b**). **4a** undergoes decarbonylation at 75° to give a mixture of acetylpentacarbonylmanganese(I) (**2a**) and methylpentacarbonylmanganese(I). The rate of decarbonylation of **4a** is 21 times slower than that of **2a** at 75°. Less than 0.3% **4a** is in equilibrium with **2a** at 85° and 110 atm of CO. Ligand substitution of **2a** via $CH_3COMn(CO)_4$ (**1**) is calculated to be over 77 500 faster than ligand substitution of **2a** via $CH_3COCOMn(CO)_4$ (**3**).

Since their discovery in 1957, alkyl- and acylpentacarbonylmanganese(I) compounds have served as convenient models for the study of the carbonylation, decarbonylation, and ligand substitution reactions of metal carbonyl compounds.[1] The carbonylation of $CH_3Mn(CO)_5$ to give $CH_3COMn(CO)_5$ has been extensively studied[1,2] and shown to occur by a methyl-migration mechanism.[2] Presumably, the reaction of other nucleophiles with $CH_3Mn(CO)_5$ to give $CH_3COMn(CO)_4L$ also proceeds by a methyl-migration mechanism. On the other hand, reaction of triphenylphosphine with $CH_3COMn(CO)_5$, which follows first-order kinetics, has been proposed to occur by a dissociative mechanism (eq 1) involving the coordinatively unsaturated intermediate **1**.[2] However, an acetyl migration mechanism (eq 2), analogous to the methyl-migration

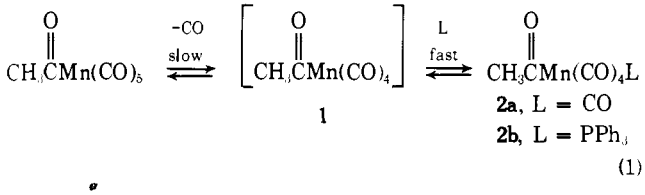

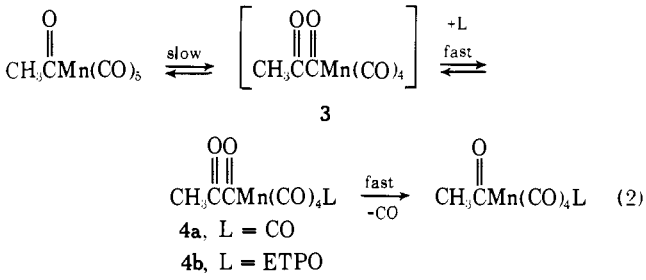

mechanism and involving the unsaturated pyruvoyl species **3**, is also in agreement with previous data.[1,2] The observation that $CH_3{}^{13}COMn(CO)_5$ reacts with $P(C_6H_5)_3$ to give $CH_3{}^{13}COMn(CO)_4P(C_6H_5)$ rules out a mechanism involving slow decarbonylation to give $CH_3Mn(CO)_5$ which then rapidly reacts with ligand to give $CH_3COMn(CO)_4L$. The direct displacement of CO by the entering ligand is inconsistent with the observed first-order kinetics.

Our interest in mechanism 2 has prompted a study of the synthesis and the kinetic and thermodynamic stability of pyruvoylpentacarbonylmanganese(I) (**4a**).[3] Here we report that **4a** undergoes decarbonylation 21 times more slowly than $CH_3COMn(CO)_5$ even though it is thermodynamically ≥4.2 kcal less stable than $CH_3COMn(CO)_5$.

Results

Pyruvoylpentacarbonylmanganese(I) (**4a**) was prepared in 33% yield from pyruvoyl chloride and $NaMn(CO)_5$ in THF at 0° and purified by vacuum sublimation as a bright red solid. The structure of **4a** was established by spectral means and confirmed by x-ray crystallography. The NMR spectrum in benzene-d_6 consists of a single sharp singlet at δ 1.63. The infrared spectrum of **4a** in heptane exhibits five bands in the metal carbonyl stretching region at 2119 w, 2055 w, 2026 vs, 2010 s, and 1990 w cm^{-1} and three bands in the acyl region at 1719, 1642, and 1600 cm^{-1}.[4a] Laser Raman data (powder) show only three peaks for CO stretching at 2118, 2044, and 1996 cm^{-1} (Table II) and the same acyl stretching bands observed by ir spectroscopy, 1708, 1636, and 1597 cm^{-1}. In addition, strong bands at 573 and 400 cm^{-1} were observed and assigned to Mn-CO bending and Mn-C stretching, respectively.[4b] The uv-visible spectrum of **4a** contains three maxima at 218 (ϵ 31 200), 255 (shoulder, ϵ 12 000), and 477 nm (ϵ 62). The red color of **4a** is apparently due to the pyruvoyl chromophore since $CH_3COMn(CO)_5$ shows no long wavelength absorption but biacetyl, a yellow compound, has a λ_{max} at 420 nm (ϵ 19).[5] Although the parent ion ($M^{\cdot+}$, *m/e* 266) was not observed, the usual fragmentation pattern for $XMn(CO)_5$ compounds was noted.[6] The major difference between the mass spectra of **4a** and $CH_3COMn(CO)_5$[6] was the greater abundance of $Mn(CO)_{6-x}{}^+$ relative to $CH_3COMn(CO)_{5-x}{}^+$ found in the spectrum of **4a**. The latter ions are very low in abundance in **4a** (4%) whereas the $Mn(CO)_{6-x}{}^+$ ions are 10-36% of the base peak. The mass spectrum of $CH_3COMn(CO)_5$ contains both types of ions in similar abundance (10-40%).[6]

The x-ray crystal structure of **4a** is shown in Figure 1. Five carbonyls and the pyruvoyl moiety are octahedrally coordinated about the manganese atom. As in all previous structural studies on $Mn(CO)_5$ units, the equatorial carbonyl groups are seen to bend away slightly from the axial carbonyl ligand.[7] The C_{ax}-Mn-C_{eq} angles vary from 92.2 to 93.5°, and the manganese atom is displaced at 0.094 Å from the plane of the equatorial carbonyl carbon atoms. This is similar to the 0.13 Å displacement found in *cis*-CHF=CFMn(CO)$_5$.[8] In addition, there is a notable lack of any difference between axial and equatorial bond lengths, with all CO groups having normal Mn-C and C-O distances.

In the pyruvoyl fragment, the acyl carbonyls are in an s-trans conformation, as seen also in chloro(methoxalyl)bis(triphenylphosphine)palladium ($L_2ClPdCOCO_2Me$) (**5**).[9]

Table I. Ir Data

Compound	Absorptions (cm^{-1})
4a[a]	2119 w, 2055 sh, w, 2026 vs, 2010 s, 1990 sh, w, 1719 w, 1642 w, 1600 w
7[a]	2120 w, 2058 sh, w, 2029 vs, 2012 s, 1700 vw, 1620 vw
9[a]	2118 m, 2058 w, 2028 s, 2022 s, 2010 s, 1682 w, 1633 w, 1620 sh, w
4b[b]	2090 m, 2018 sh, s, 2004 vs, 1989 sh, s, 1690 w, 1640 w, 1585 w
4b (red)[c]	2085 s, 2016 s, 1987 br, s, 1715 m, 1632 w, 1582 s, 1030 s, 945 s, 810 s, 795 s, 775 m, 670 m, 635 s
4b (yellow)[c]	2090 s, 2020 s, 1990 br, s, 1712 sh, w, 1695 m, 1632 w, 1585 s, 1035 s, 955 s, 805 s, 775 s, 685 s, 640 s, 633 sh, s

[a] In heptane, [b] Either red or yellow crystalline form in chloroform. [c] KBr pellet.

Table II. Raman Data (powder)

Compound	Absorptions (cm^{-1})
4a	2118 w, 2044 s, 1996 m, 1708 vw, 1636 w, 1597 w, 573 s, 400 vs, 270 s, 190 s
7	2121 m, 2055 s, 2005 s, 1996 sh, m, 1667 w, 1612 sh, w, 1595 s, 1000 s, 715 w, 689 w, 650 w, 615 w, 598 s, 445 m, 399 vs, 330 vs, 290 vs
4b (red)	2081 s, 2018 vs, 1998 m, 1975 vs, 1715 w, 1583 m, 782 s, 648 s, 570 m, 460 s, 434 s, 419 s, 269 s
4b (yellow)	2091 s, 2020 vs, 1985 vs, 1698 w, 1585 m, 780 m, 648 s, 458 m, 418 vs, 307 s, 265 m

The longer Mn–C distance (2.075 (4) Å) expected for a σ-bond with little π back-donation is similar to that found for $CF_3CF_2COMn(CO)_5$, 2.047 (12) Å.[10] The carbon–carbon and carbon–oxygen distances within the pyruvoyl segment are normal and the carbon–oxygen distances are in agreement with those found in **5**.[9] The pyruvoyl group is twisted slightly out of planarity: the angle between the planes of the acyl carbonyls is 10.4° (Table 11).[29] Nonbonding repulsions between the pyruvoyl and $Mn(CO)_5$ groups are minimized by the staggered relationship between the pyruvoyl ligand and the equatorial carbonyl ligands: the angle between the [Mn, C(6), O(6), C(7)] plane and the [Mn, C(1), C(3), C(4), C(6)] plane is 44.2°.

4a reacted with a 50% excess of 4-ethyl-2,6,7-trioxa-1-phosphabicyclo[2.2.2]octane, ETPO, in refluxing benzene for 1 h to give the substitution product, **4b**. Column chromatography gave 20% recovery of **4a**[18] and 32% yield of **4b**

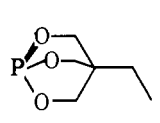

ETPO

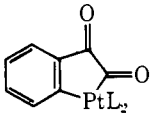

6

(based on recovered **4a**). **4b** crystallized as a mixture of red and yellow crystals which were separated manually. The red crystalline form is apparently less thermodynamically stable since these crystals turn yellow just before melting. A similar phenomenon was noted in the conversion of blue **6** to red **6** prior to melting.[11] Qualitatively the red crystals appear to be less soluble than the yellow crystals.

Spectral analysis of *cis*-$CH_3COCOMn(CO)_4$(ETPO) (**4b**) proved interesting since both the red and yellow crystals obtained in the preparation of **4b** gave the same solution spectra. The NMR of either crystal form in $CDCl_3$ exhibits a doublet (J_{P-H} = 4 Hz) at δ 4.29, a quartet (J = 7 Hz) at δ 1.27, and a triplet (J = 7 Hz) at δ 0.84 for the ETPO ligand. The methyl resonance of the pyruvoyl moiety was found as a singlet at δ 2.03. The solution ir spectrum of the red or yellow crystals showed bands at 2090, 2018, 2004, and 1989 cm^{-1} for the metal carbonyl stretching vibrations consistent with a cis configuration.[12] When the solid-state ir or Raman spectra were obtained differences were evident, however. The Raman spectra showed four metal carbonyl bands at 2081, 2018, 1998, and 1975 cm^{-1} for the red crystals and three bands at 2091, 2020, and 1985 cm^{-1} for the yellow ones. The acyl bands are found at 1715 and 1583 cm^{-1} for red **4b** and at 1698 and 1585 cm^{-1} for the yellow form of **4b**. In addition, bands at 570 and 434 cm^{-1} in the spectrum of the red crystals are absent in the spectrum of yellow **4b**, which contains a peak at 307 cm^{-1} missing from the spectrum of red **4b**. No maximum was observed in the uv-visible spectra at >250 nm in chloroform for either crystalline form. As expected, the mass spectra of both red and yellow **4b** were very similar, the highest mass peak in both cases being $M^{\cdot+} - 43$, *m/e* 358. In view of these results and similar behavior reported for **6**, where x-ray data have indicated conformational isomers via twisting about the two carbonyl groups, it is reasonable to conclude that the red and yellow forms of **4b** are conformational isomers which can be interconverted in solution by rotation about the CO–CO bond of the pyruvoyl moiety.

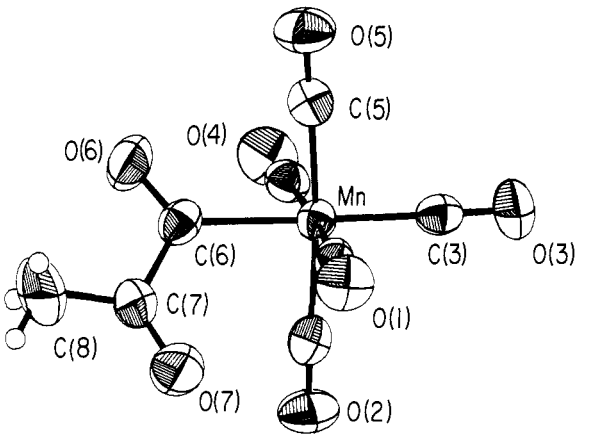

Figure 1. ORTEP drawing of the molecular structure of MeCOCOMn$(CO)_5$, **4a**, with thermal ellipsoids (50% probability).

Phenylpyruvoylpentacarbonylmanganese(I) (**7**)[13] was

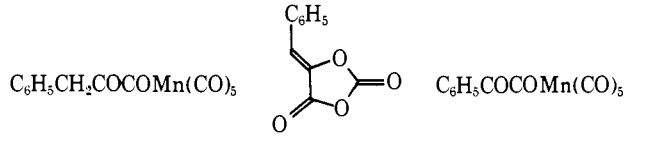

7 **8** **9**

synthesized by a less direct route due to the instability of phenylpyruvoyl chloride. Benzylidene-1,3-dioxolan-2,4-dione (**8**), which has been used to prepare derivatives of phenylpyruvic acid,[14] was employed as a precursor of **7**. Thus, reaction of equimolar amounts of **8** and $NaMn(CO)_5$ at 25° gave, after column chromatography, a 23% yield of red solid identified as **7** by spectral data.

The NMR spectrum of **7** in acetone-d_6 exhibited a broad singlet (δ 7.23) and a sharp singlet (δ 3.82). This compares with δ 7.23 and 4.24 for the related compound $PhCH_2COMn(CO)_5$ in the same solvent.[15] The close similarity of the ir spectrum of **7** to that of **4a** is striking in the metal carbonyl region. Four bands are seen at 2120, 2058 (shoulder), 2029, and 2012 cm^{-1} consistent with the $Mn(CO)_5$ group. Two weak acyl bands at 1700 and 1620 cm^{-1} are also present. The electronic absorption spectrum shows maxima at 218 (ϵ 37 000), 255 (sh, ϵ 12 000), and 458 nm (ϵ 116), very similar to that of **4a**.

Similarly, benzoylformylpentacarbonylmanganese(I) (**9**)

Table III. Rates of Decarbonylation of $RCOMn(CO)_5$ in Benzene

Compound	Temp, °C	$10^5 k$ (sec^{-1})
$CH_3COCOMn(CO)_5$, 4a	88.0[a,b]	53.5 ± 3.3
4a	84.5[a,b]	39.0 ± 2.1
4a	79.5[a,b]	21.2 ± 1.1
4a	73.0[a,b]	10.9 ± 0.9
4a	69.0[a,b]	7.05 ± 0.82
4a	50.87[c]	0.376 ± 0.027
$PhCH_2COCOMn(CO)_5$, 7	72.5[a]	9.31 ± 1.40
$CH_3COMn(CO)_5$, 2a[d]	75.0[e]	283.

[a] Temperatures were estimated from the NMR peak separations of ethylene glycol and are accurate to ±1.0. Temperature control was to ±0.2°. [b] $\Delta H^{\ddagger}$ = 25.3 ± 2.0 kcal mol^{-1} at 75°. [c] Temperature measured with a high precision thermometer in constant temperature bath and is accurate to ±0.02°. [d] Rate determined by NMR analysis of aliquots taken from an open system periodically flushed with nitrogen. [e] Temperatures were measured in an oil bath with a high precision thermometer and are accurate to ±0.2°.

was prepared from a solution of benzoylformyl chloride and $NaMn(CO)_5$ in THF at 0°. Recrystallization of the crude reaction product gave a 92% yield of **9** as orange plates.

The NMR spectrum of **9** displayed two multiplets in the aromatic region (δ 7.96, 2 H, and 7.68, 3 H). Both the ir and Raman spectra are consistent with the proposed structure; in heptane solution five bands were seen in the metal carbonyl region at 2118, 2058, 2028, 2022, and 2010 cm^{-1} as well as three bands in the acyl stretching region at 1682, 1633, and 1620 cm^{-1}.[4a] The Raman spectrum (powder) has strong bands at 598 and 399 cm^{-1} which supports our assignment of similar bands in the spectrum of **4a** as Mn-C-O bending and Mn-C stretching, respectively. The uv-visible spectrum of **9** (heptane) had a long wavelength band at 438 nm (ϵ 273), responsible for the orange-red color of its solutions, and additional maxima at 208 (ϵ 38 300) and 253 nm (ϵ 19 100).

Kinetic Studies. The thermal decomposition of $CH_3COCOMn(CO)_5$, **4a**, in benzene was studied by NMR. The reaction was followed by measuring the disappearance of the singlet at δ 1.63 using *p*-di-*tert*-butylbenzene as an internal standard. When the decomposition was carried out in a sealed tube, the products of the reaction were an equilibrium mixture of $CH_3COMn(CO)_5$, **2a** (singlet at δ 2.18), and $CH_3Mn(CO)_5$ (singlet at δ −0.26). At the end of the reaction, the CO pressure in the tube was calculated to be ~2 atm. The inhibition of the rate of decomposition of **4a** by CO in this pressure range must be very small since no deviation from first-order kinetics was observable when the reaction was carried to 87% completion. However, there may be some slight CO inhibition since, at 110 atm of CO, the rate of decarbonylation of **4a** was retarded (vide infra). At 75°, the rate of decomposition of **4a** is 21 times slower than the rate of decarbonylation of **2a** in benzene (Table III). The thermal decarbonylation of $PhCH_2COCOMn(CO)_5$, **7**, proceeded at approximately the same rate as **4a**. The phenyl group is apparently too far removed to affect the rate.

The rate of decarbonylation of **4a** was compared with the rate of substitution by ETPO. The ETPO substitution reaction was followed by observing the disappearance of the high frequency band (2119 cm^{-1}) in the metal carbonyl region of **4a**. The rate of reaction of **4a** with ETPO at 50.87° to give **4b** is 1.2 times faster than the rate of decarbonylation of **4a** at the same temperature (Table IV). It is not clear whether this rate difference is within experimental error or due to slight CO inhibition of the rate of decarbonylation of **4a**. The rate of substitution is independent of ligand concentration. At 50.8°, the rate of ETPO substitution of $MeCOMn(CO)_5$, **2a**, was found to be about 100 times faster than the rate of substitution of **4a**.

Table IV. Rates of Substitution Reactions with ETPO at 50.87° ± 0.02

Compound	Concn	[ETPO]	$10^6 k$ (sec^{-1})
$CH_3COCOMn(CO)_5$, 4a	0.059	0.104	4.64 ± 0.27
4a	0.061	0.232	4.58 ± 0.23
$CH_3COMn(CO)_5$, 2a	0.061	0.101	492. ± 30

$$CH_3CMn(CO)_5 + CO \rightleftharpoons CH_3CCMn(CO)_5 \quad (3)$$

Several attempts were made to measure the amount of **4a** in equilibrium with **2a** at high CO pressure. No detectable amount of **4a** was observed when a solution of **2a** was heated to 80° for 9 h under 258 atm of CO. This could be due either to an unfavorable equilibrium or to a kinetically slow approach to equilibrium. Attempts were also made to achieve equilibrium beginning with **4a**. The rate of decarbonylation of **4a** to give **2a** was found to be somewhat slower at high CO pressure than in the absence of external CO pressure. A benzene solution of **4a** was heated to 85° for 8 h under 110 atm of CO; analysis of the reaction mixture by 270-MHz ^1H NMR operating in the Fourier transform mode indicated that the reaction mixture contained 2.6% **4a** in addition to **2a**. From kinetic studies carried out in the absence of added CO pressure, <0.002% **4a** would have been expected. Thus, a high pressure of CO inhibited the decarbonylation of **4a**. In a similar experiment, a benzene solution of **4a** was heated to 85° for 30 h under 110 atm of CO. On the basis of the 8-h experiment less than 0.00004% **4a** would have been expected. However, Fourier transform 270-MHz NMR indicated a singlet at δ 1.63 possibly due to **4a** which was 0.3% as intense as the singlet due to **2a**. Although there is no other evidence to confirm the tentative NMR assignment, the *maximum* amount of **4a** in equilibrium with **2a** at 110 atm is 0.3%. The concentration of CO in benzene at 85° under 110 atm of CO pressure is estimated to be about 1.2 M.[16,17] Using this value for [CO], the K_{eq} at 85° for reaction 3 is calculated to be $\leq 2.5 \times 10^{-3}$ M^{-1} and the ΔG at 85° for reaction 3 is calculated to be ≥4.2 kcal mol^{-1}. Therefore **4a** is thermodynamically less stable but kinetically more stable than **2a**.

Discussion

Our studies of $CH_3COCOMn(CO)]_5$ were initiated to explore the possibility that ligand substitution reactions of acetylmanganese compounds might proceed via acetyl migration to give pyruvoylmanganese compounds as unstable intermediates. Our discovery that **4a** possesses high kinetic stability precludes the intermediacy of such compounds as intermediates in the substitution reactions of acyl manganese compounds. The rate of decarbonylation of **4a** at 75° was found to be 21 times slower than that of $CH_3COMn(CO)_5$.

Two mechanisms for the decarbonylation of **4a** were considered: first, concurrent loss of CO and acyl migration might produce $CH_3COMn(CO)_5$ directly (route A); alternatively, loss of CO might produce a coordinatively unsaturated intermediate which could subsequently undergo acetyl migration (route B). In an attempt to trap the coordinatively unsaturated intermediate **3**, the reaction of **4a** in the presence of ETPO was studied. The formation of an ETPO substitution product is consistent with the intervention of a coordinatively unsaturated intermediate. The rate of ETPO substitution of **4a** was only 1.2 times faster than the rate of

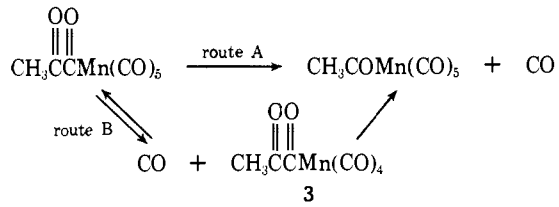

decarbonylation and did not depend on the concentration of the incoming ligand (Table IV). This small rate difference may be due either to experimental error or to a slight CO inhibition. Therefore the decarbonylation and substitution reactions of **4a** both involve loss of a CO ligand as the slow step. Similar results were reported for the reaction of MeCOMn(CO)$_5$ with several nucleophiles in bis(2-ethoxyethyl) ether at 30.5°.[18]

Examination of route B indicates that inhibition by CO might be observable. Since no curvature was observed in rate plots of the decarbonylation of **4a** in sealed tubes in which the CO pressure rose to 2 atm during the reaction, the CO inhibition cannot be large. The fact that decarbonylation of **4a** in sealed tubes was 1.2 times slower than ETPO substitution may be due to slight CO inhibition of decarbonylation. At 110 atm of CO, a retardation in the rate of decarbonylation was observed.

Attempts to equilibrate **4a** and **2a** led to the predominant conversion of **4a** to **2a** even under 110 atm of CO. A limit on the maximum amount of **4a** in equilibrium with **2a** under 110 atm of CO was put at 0.3%. This corresponds to $K_{eq} \leq 2.5 \times 10^{-4}$ and $\Delta G \geq 4.2$ kcal mol^{-1} for eq 3. Interestingly, while **4a** is kinetically 21 times more stable than **2a**, it is thermodynamically 400 times less stable than **2a**.

Initially we were interested in determining the relative importance of reactions 1 and 2 in the substitution reactions of CH$_3$COMn(CO)$_5$, **2a**. Since we now know that the ligand substitution reactions of **4a** proceed by intermediate **3** and since we can place limits on the equilibrium constant between **2a** and **4a**, we can now construct a free energy diagram showing the relative free energies of CH$_3$Mn(CO)$_5$, CH$_3$COMn(CO)$_5$, CH$_3$COCOMn(CO)$_5$, and the free energies of activation for the interconversion of these compounds via CH$_3$COMn(CO)$_4$, **1**, and CH$_3$COCOMn(CO)$_4$, **3** (Figure 2). The rate of ETPO substitution of **2a** and **4a** at 50.87° was used to determine $\Delta G^{\ddagger}$ for formation of intermediates **1** and **3**, respectively. The ΔG between **4a** and **2a** was found to be ≥4.2 kcal mol^{-1} at 85° in this study; at 50°, the free energy differences would be expected to be somewhat greater since ΔS should be positive for a reaction bringing two molecules together. For the related reaction of CH$_3$Mn(CO)$_5$ with CO to give CH$_3$COMn(CO)$_5$, ΔS = +30. The free energy difference between CH$_3$COMn(CO)$_5$ and CH$_3$Mn(CO)$_5$ at 50° was calculated to be 2.9 kcal from the data in β,β'-diethoxyethyl ether of Calderazzo and Cotton.[19]

Inspection of Figure 2 allows the estimation that the free energy of activation for the formation of CH$_3$COCOMn(CO)$_4$, **3**, from **2a** is ≥7.2 kcal mol^{-1} higher than the free energy of activation for the formation of CH$_3$COMn(CO)$_4$, **1**, from **2a**. This corresponds to a rate preference for the formation of **1** from **2a** of over 77 500. Not only is the formation of **1** from **2a** the major pathway for substitution reactions of **2a** but the alternate route via acyl migration to **3** is of substantially higher energy. Acyl migration should be considered a highly unlikely route in the substitution reactions of acylmetal compounds.

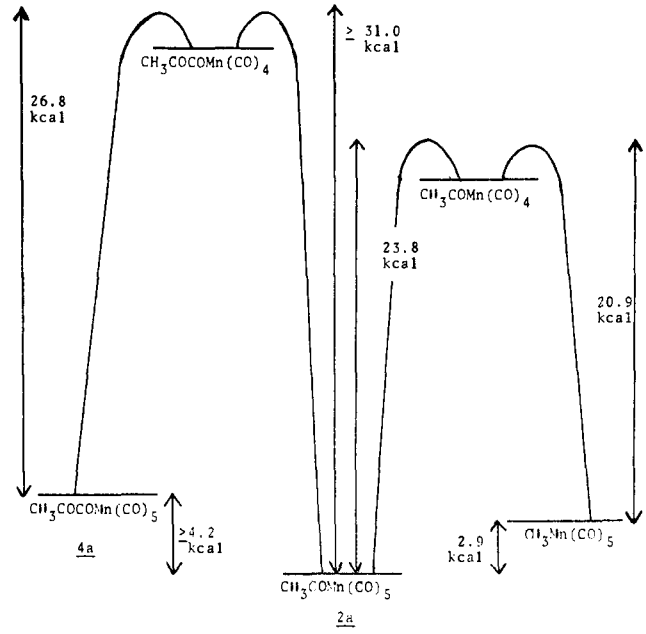

Figure 2. Free energy diagram showing the relative free energies of CH$_3$Mn(CO)$_5$, CH$_3$COMn(CO)$_5$, and CH$_3$COCOMn(CO)$_5$ and the $\Delta G^{\ddagger}$ for the interconversion of these compounds via MeCOMn(CO)$_4$ and MeCOCOMn(CO)$_4$ at 50.8°.

Experimental Section

General. Infrared spectra were recorded on a Dilgilab FTS-20 Fourier transform interferometer, a Beckman IR-8 spectrophotometer, and a Perkin-Elmer 267 spectrophotometer. The laser Raman spectra were recorded on a Spex Ramalog spectrometer. Ultraviolet-visible (uv-visible) spectra were recorded either on a Cary 15 spectrophotometer or on a Beckman DK-2A spectrophotometer. NMR spectra were recorded on Varian A60A (60 MHz), Jeol MH100 (100 MHz), Varian XL-100 (100 MHz), or Brucker WH-270 (270 MHz) spectrometers. Mass spectra were run on an AEI-MS902 spectrometer at 70 eV except for gc-mass spectra which were recorded on a Varian CH-7 mass spectrometer. Melting points are uncorrected. Elemental analyses were obtained from Galbraith Laboratories, Inc., Knoxville, Tenn.

Solvents were purified by distillation under nitrogen from the usual drying agents. Reactions were carried out under a nitrogen atmosphere.

Pyruvoyl Chloride. Following the method of Carre and Jullien,[20] 35 ml (432 mmol) of pyridine in 50 ml of ether was added dropwise to a cooled (0°) solution of 85% pyruvic acid (43.7 g, 432 mmol) and thionyl chloride (39.2 ml, 540 mmol) in 80 ml of ether. Large amounts of solid formed and a mechanical stirrer was necessary to maintain adequate stirring. After filtering the mixture, solvent was removed by distillation at −25° (1 mm) and product was distilled at 25° (1 mm) into a trap at −78° giving a mixture of 64% CH$_3$COCOCl (6.4 g, 60 mmol), 24% SOCl$_2$, and 22% ether by weight which was used without further purification. The amounts were determined by NMR using a sample containing a specified weight of chloroform.

Pyruvoylpentacarbonylmanganese(I), 4a. NaMn(CO)$_5$ (95 ml, 0.62 M, 59 mmol) in THF was added to the mixture of pyruvoyl chloride prepared above at 0°. The dark red solution was stirred for 15 min and the solvent removed on a rotary evaporator. Bright red crystals (5.27 g, 19.8 mmol, 33%) were collected by sublimation at 25° (0.2 mm). Recrystallization from ether-pentane at −78° gave red crystals of **4a**: mp 76–77°; mass spectrum: *m/e* (intensity), no M·$^+$, 238(0.2), 223(12.8), 210(1.1), 195(16.5), 182(2.1), 167(13.2), 154(1.0), 139(24.0), 126(3.6), 111(29.4), 98(21.8), 83(36.0), 70(11.0), 55(100), and 43(31.0).

Anal. Calcd for C$_8$H$_3$MnO$_7$: C, 36.09; H, 1.13; Mn, 20.68. Found: C, 36.38; H, 1.38; Mn, 20.3.

Preparation of CH$_3$COCOMn(CO)$_5$(ETPO), 4b. A solution of **4a** (332 mg, 12.5 mmol) and ETPO (307 mg, 1.89 mmol) in 10 ml of benzene was refluxed 1 h. Column chromatography (silica gel-chloroform) gave an initial red band consisting of **4a** (66 mg) followed by an orange band containing **4b** (127 mg, 0.32 mmol, 32% based on recovered **4a**) which was obtained as a mixture of yellow and red crystals upon evaporation of solvent. The crystals were

separated by physical means; however, spectral properties of the solutions of either the yellow or red crystals were the same: uv ($CHCl_3$) no maximum >250 nm, 375 (ϵ 114) nm; NMR ($CDCl_3$) δ 4.29 (6 H, d, J_{PH} = 4 Hz), 2.03 (3 H, s), 1.27 (2 H, q, J = 7 Hz), and 0.84 (3 H, t, J = 7 Hz); (acetone-d_6) δ 4.43 (6 H, d, J_{PH} = 4.5 Hz), 1.94 (3 H, s), 1.38 (2 H, q, J = 7 Hz), and 0.86 (3 H, t, J = 7 Hz). Mass spectral analysis of the red and yellow crystals of **4b** gave the following respective *m/e*: no $M^{\cdot+}$, 358 (2.3), 357 (18.9), 344 (7.1), 330 (3.6), 329 (13.9), 316 (0.2), 301 (2.3), 288 (4.1), 274 (3.2), 273 (33.3), 260 (15.0), 245 (17.1), 233 (4.6), 232 (57.4), 218 (14.6), 217 (100), 202 (2.9), 187 (2.2), 162 (5.2), 149 (3.6), 132 (10.4), 118 (23.3) and no $M^{\cdot+}$, 357 (13.8), 344 (4.4), 329 (8.7), 316 (1.0), 301 (2.2), 288 (4.1), 274 (2.4), 273 (24.8), 260 (12.4), 245 (14.5), 233 (4.3), 232 (51.6), 218 (8.7), 217 (100), 202 (4.4), 187 (3.3), 174 (3.8), 162 (4.5), 149 (6.6), 132 (12.6), 118 (61.8).

In contrast to their solution behavior, the yellow and red crystals exhibit different solid-state properties (See Tables I and II for ir and Raman data).

Yellow crystals of **4b**: mp 84–85°.

Red crystals of **4b**: mp 82–83°. (The red crystals appear to turn yellow at approximately 80°.)

Anal. Calcd for $C_{13}H_{14}MnO_9P$ (red crystals): C, 39.02, H, 3.53; Mn, 13.73; P, 7.74. Found: C, 38.98; H, 3.67; Mn, 13.69; P, 7.74.

Preparation of *cis*-$CH_3COMn(CO)_4ETPO$. Following a procedure similar to that of Green,[21] $CH_3Mn(CO)_5$ (388 mg, 1.8 mmol) and ETPO (290 mg, 1.8 mmol) were stirred in 15 ml of THF at 25° for 3 hr. Most of the solvent was evaporated and 10 ml of pentane was added. Upon cooling to 0° a white solid precipitated. Concentration gave additional *cis*-$CH_3COMn(CO)_4ETPO$ (467 mg, 70%); mp 154–157° (dec), lit.[21] 155–156°.

Preparation of Phenylpyruvoylpentacarbonylmanganese(I) (7). 8 (4.7 g, 24.8 mmol) in ether and an equimolar amount of $NaMn(CO)_5$ in THF were stirred together at 25° for 30 min and then quenched with water. Column chromatography (20:80 ether–benzene) gave a red solid, which was further purified by recrystallization from ether at −78° to give **7** (1.3 g, 15%): mp 62.5–63.5°.

Benzoylformyl Chloride. Benzoylformyl chloride (2.95 g, 17.5 mmol, 67%) was prepared from 3.9 g (26 mmol) of benzoylformic acid, and 9.9 g (78 mmol) of oxalyl chloride according to the procedure of Kharasch and Brown.[22] The product was collected by distillation, bp 49–51° (1 mm).

Benzoylformylpentacarbonylmanganese(I) (9). $NaMn(CO)_5$ (12 ml, 1.1 M, 13.2 mmol) in THF was added to a stirred solution of 2.95 g (17.5 mmol) of benzoylformyl chloride and 10 ml of THF at 0°. The bright red solution was stirred at 0° for 30 min and 10 ml of water was added. The layers were separated, and the water layer was extracted with 10 ml of pentane. Evaporation of solvent from the dried organic layer gave a red-orange oil which solidified upon cooling. Recrystallization of 4.6 g of this crude material from ether–heptane gave 4.0 g (12.2 mmol, 92%) of orange flakes of **9**; mp 61.5–62.5°.

Anal. Calcd for $C_{13}H_5MnO_7$: C, 47.56; H, 1.52. Found: C, 48.16; H, 1.61.

Measurement of the Rate of Decarbonylation of $CH_3COMn(CO)_5$, 4a, and $PhCH_2COCOMn(CO)_5$, 7. Samples for NMR rate studies consisted of 40–50 mg of **4a** or **7**, 5–6 mg of *p*-di-*tert*-butylbenzene, and 0.3–0.5 ml of benzene. The samples were degassed and sealed under vacuum. A Varian A-60A variable temperature NMR spectrometer was employed in the rate studies. The probe temperature was measured before and after each experiment by the chemical shift difference of the ethylene glycol resonances. The reactions were monitored by integration over the methyl absorption of **4a** at δ 1.63 and internal standard (δ 1.21). Each point was determined from the average of at least three separate integrations.

The decarbonylation of **7** was followed by integration over the methylene resonance (δ 3.55) and the standard peak (δ 1.21). The products were $PhCH_2COMn(CO)_5$ (δ 3.86) and $PhCH_2Mn(CO)_5$ (δ 2.33). Results are shown in Table III.

An additional experiment was carried out with **4a** as above except the sealed NMR tube containing the sample was warmed in a constant temperature bath (50.87 ± 0.02°). The tube was removed periodically and immediately cooled in dry ice–acetone. The spectra were recorded at ambient temperature (35°) on a Joel MH100 instrument. The disappearance of **4a** was followed by the average ratio (**4a**/std) of these three separately recorded ratios.

Rate of the Decarbonylation of $CH_3COMn(CO)_5$. To avoid CO inhibition an open system under nitrogen was used along with a rapidly stirred oil bath. Temperatures measured with a high precision thermometer were constant to ±0.2° during the runs. Aliquots were taken from a solution of $CH_3COMn(CO)_5$ and *p*-di-*tert*-butylbenzene in degassed benzene and were frozen immediately in NMR tubes. The disappearance of $CH_3COMn(CO)_5$ was monitored by integrating (at least three times) over the methyl signal and the *tert*-butyl singlet of the standard. Each run consisted of six–ten points.

Rate of Substitution of $CH_3COCOMn(CO)_5$, 4a, and $CH_3COMn(CO)_5$ with ETPO. Samples were prepared in degassed benzene and sealed in vacuo. The samples were immersed in a constant temperature bath at 50.87 ± 0.02°. The reactions were quenched at −78° and stored at −25° until ir analysis could be obtained. A Perkin-Elmer 267 grating spectrophotometer was used with the frequency scale expanded five times. The disappearance of the 2119 and 2117 cm^{-1} bands were followed for **4a** and $CH_3COMn(CO)_5$, respectively. Rates (Table IV) are based on a single run of six points with each point being determined by the average of at least three scans. The reactions were first order to >65% completion for **4a** and >80% completion for $CH_3COMn(CO)_5$. A linear dependence on Beer's law was found in the concentration range used. Examination of the ir spectrum of the samples indicated only one product was formed in each case; however, TLC analysis indicated a very small amount of bissubstitution product in both cases.

Decarbonylation of 4a under 110 Atm of CO. $CH_3COCOMn(CO)_5$, **4a** (114 mg, 0.428 mmol), in benzene (3 ml) was heated (85°) under 110 atm of CO for 8 h. A 100-MHz NMR of the filtered solution after addition of *p*-di-*tert*-butylbenzene (8.0 mg, 0.042 mmol) indicated the following materials present: $CH_3COMn(CO)_5$ (0.285 mmol, 64%), $CH_3COCOMn(CO)_5$ (0.011 mmol, 2.6%), $CH_3Mn(CO)_5$ (0.021 mmol, 4.9%), $CH_3COMn(CO)_5$/**4a** = 27/1 = 96.4/3.6.

Another experiment was carried out with **4a** (31 mg, 0.12 mmol) and benzene-d_6 (0.9 ml) at 85° and 110 atm of CO for 30 h. None of **4a** could be detected by conventional 100-MHz NMR as the sample was contaminated with oil. Since **4a** and $CH_3COMn(CO)_5$ have the same R_f on silica gel eluted with 5:95 ether–hexane, both would be collected from the same TLC band. Preparative TLC afforded 14.4 mg (0.06 mmol, 50%) of $CH_3COMn(CO)_5$ which was examined by 270-MHz Fourier transform NMR. A signal corresponding to the expected location for **4a** was detected and found to be 0.3% of the intensity (by peak height) of $CH_3COMn(CO)_5$.

X-Ray Crystal Structure of 4a. Data Collection and Reduction. Red crystals of **4a** were obtained by sublimation at room temperature and 20 mm. The needle-like crystal of trapezoidal cross-section with dimensions (each defined by the perpendicular distance from a common origin within the crystal) 0.112 (00$\bar{1}$), 0.112 (001), 0.255 (10$\bar{1}$), 0.065 ($\bar{1}$10), 0.255 (0$\bar{1}$1), and 0.065 mm (1$\bar{1}\bar{1}$) was wedged in a glass capillary, sealed in air, and placed on a Syntex P$\bar{1}$ computer controlled diffractometer equipped with a graphite monochromated Mo Kα radiation source. The preliminary Syntex routines[23] indicated a primitive monoclinic cell with dimensions a = 6.320 (3) Å, b = 6.340 (3) Å, c = 29.971 (13) Å, γ = 119.48 (3)°, and V = 1045.3 (8) Å^3. The $2/m$ (C_{2v}) Laue symmetry was verified by partial rotation photographs along two of the reciprocal axes. The experimental density of 1.66 g cm^{-3}, determined by flotation in aqueous $ZnCl_2$, agrees with 1.68 cm^{-3}, calculated on the basis of Z = 4.

A total of 1806 diffraction maxima were collected from 3° ≤ 2θ ≤ 40° through four octants ($\pm h$, $\pm k$, l) by the variable 2θ–ω scan speed technique. The mean deviation of the intensities of the two standard peaks, monitored after every 50 reflections, was 3% and appeared random. The intensities were reduced and merged in the usual fashion[24] to yield 775 independent reflections for which $I > 2\sigma(I)$.[25] Later, the data were corrected for crystal absorption effects. With the linear absorption coefficient, ν = 13.42 cm^{-1}, the transmission factors varied from 0.72 to 0.81. The observed systematic absences for $hk0$ ($h + k = 2n + 1$) and $00l$ ($l = 2n + 1$) uniquely define the space group as $P2_1/n$ (nonstandard setting of $P2_1/b$, no. 14 C^5_{2c}).[26]

Solution and Refinement. The structure was determined using

the standard heavy atom method.[27] The observed molecular structure and crystallographic packing neatly explain the observed near-hexagonal lattice parameters. Full-matrix isotropic least-squares refinement converged at R_1 = 6.0% and R_2 = 8.8%.[28] At this stage, a difference Fourier map revealed coordinates for the methyl hydrogen atoms. These were included as fixed-atom contributions (β = 7.0 Å^2) in the final anisotropic refinement series to yield R_1 = 2.7% and R_2 = 3.6%. No attempt was made to refine the hydrogen atom coordinates or thermal factors due to the low data/parameter ratio of 5.8:1. In the last cycle, the maximum shift in any atom parameter was 0.03σ. The final error-of-fit was 1.08. An examination of the structure factor amplitudes shows no evidence of extinction effects.

The final atomic coordinates and thermal parameters and their associated standard deviations are given in Tables 5 and 6. Bond distances and angles and selected intermolecular distances are listed in Tables 7, 8, and 9, respectively. Some selected intramolecular nonbonding distances are listed in Table 10 and some least-squares planes in Table 11. Table 12 contains the observed and calculated structure factor amplitudes.[29]

Acknowledgment. Support by the National Science Foundation through Grants GP-32160 and GP-41259X and a departmental instrument grant, which allowed the purchase of the automated diffractometer, is gratefully acknowledged.

Supplementary Material Available: atomic coordinates, thermal parameters, bond distances and angles, and structure factor amplitudes (12 pages). Ordering information is given on any current masthead page.

References and Notes

(1) For a review of CO insertion reactions see A. Wojcicki, *Adv. Organomet. Chem.*, **11**, 88 (1973).
(2) K. Noack and F. Calderazzo, *J. Organomet. Chem.*, **10**, 101 (1967).
(3) A preliminary communication has appeared: C. P. Casey and C. A. Bunnell, *J. Am. Chem. Soc.*, **93**, 4077 (1971).
(4) (a) The observation of greater than two ketonic bands may be due to rotational isomerism. Two ketonic bands are observed in $CH_2FCOMn(CO)_5$ and related compounds. F. Calderazzo, K. Noack, and U. Schaerer, *J. Organomet. Chem.*, **6**, 265 (1966); (b) A. Terzis, T. C. Strekas, and T. G. Spiro, *Inorg. Chem.*, **13**, 1346 (1974).
(5) J. C. Calvert and J. N. Pitts, Jr., "Photochemistry", Wiley, New York, N.Y., 1966, p 422.
(6) L. G. Herman, Ph.D. Thesis, Lehigh University, 1969.
(7) W. Clegg and P. J. Wheatley, *J. Chem. Soc. Dalton Trans.*, 424 (1974), and references therein.
(8) F. W. B. Einstein, H. Luth, and J. Trotter, *J. Chem. Soc. A*, 89 (1967).
(9) J. Fayos, E. Dobrzynski, R. J. Angelici, and J. Clardy, *J. Organomet. Chem.*, **59**, C33 (1973).
(10) M. R. Churchill, *Perspect. Struct. Chem.*, **3**, 126 (1970).
(11) J. A. Evans, G. F. Everett, R. D. W. Kemmitt, and D. R. Russell, *J. Chem. Soc., Chem. Commun.*, 158 (1973).
(12) D. M. Adams, "Metal-Ligand and Related Vibrations", Edward Arnold, London, 1967, p 100.
(13) We thank Yun Yu Tom for his assistance in the preparation of this compound.
(14) B. W. Dominy and R. G. Lawton, *Chem. Commun.*, 1448 (1968).
(15) K. Noack, U. Schaerer, and F. Calderazzo, *J. Organomet. Chem.*, **8**, 517 (1967).
(16) A. Seidell and W. F. Linke, "Solubilities of Inorganic and Metal Organic Compounds", Vol. I, 4th ed, D. Van Nostrand, New York, N.Y., 1958, report the solubility of CO in benzene at 1 atm over the temperature range 20–60°. Extrapolation to 85° gave a value of 0.25 ml of CO/ml of benzene at 1 atm. The solubility at 110 atm of CO was estimated using Henry's law[17] to be 27.5 ml of CO/ml of benzene or 1.22 M.
(17) The solubility of CO and H_2 in hydrocarbon solvents and in methanol follows Henry's law closely to >250 atm. S. Peter, M. Weinert, *Z. Phys. Chem. (Frankfort am Main)*, **5**, 114 (1955); S. Kruger and A. P. P. Nobel, *Recl. Trav. Chim. Pays-Bas*, **80**, 1145 (1961); R. Battino and H. L. Clever, *Chem. Rev.*, **66**, 395 (1966).
(18) F. Calderazzo and K. Noack, *Coord. Chem. Rev.*, **1**, 118 (1966).
(19) F. Calderazzo and F. A. Cotton, *Inorg. Chem.*, 1, 30 (1962).
(20) P. Carre and P. Jullien, *C. R. Acad. Sci.*, **202**, 1521 (1936).
(21) M. Green, R. I. Hancock, and D. C. Wood, *J. Chem. Soc. A*, 2718 (1968).
(22) M. S. Kharasch and H. C. Brown, *J. Am. Chem. Soc.*, **64**, 329 (1942).
(23) R. A. Sparks et al., "Operations Manual, Syntex P$\bar{1}$ Diffractometer", Syntex Analytical Instruments, Cupertino, Calif., 1970.
(24) The integrated intensity (I) was calculated according to the expression $I = [S - (B_1 + B_2)/B_R]T_R$ where S is the scan count, B_1 and B_2 are the background counts, B_R is the ratio of background time to scan time (B_R = 0.67 for this data set), and T_R is the 2θ scan rate in degrees per minute. The standard deviation of I was calculated as $\sigma(I) = T_R[S + (B_1 + B_2)/B_R^2 + q(I)^2]^{1/2}$ where q in this case was equal to 0.003.
(25) For 185 reflections $I \leq 2\sigma(I)$.
(26) "International Tables for X-Ray Crystallography", Vol. I, 2nd ed, The Kynoch Press, Birmingham, England, 1965, p 98. The coordinates of equivalent positions for $P2_1/n$ are $\pm[X,Y,Z; \frac{1}{2} - X, \frac{1}{2} - Y, \frac{1}{2} + Z]$.
(27) All crystallographic programs used in structural determination and least-squares refinement were written by one of us (J.C.C.). The absorption correction program DEAR (J. F. Blount) uses the Gaussian integration method of Busing and Levy. Plots were made using ORTEP (C. K. Johnson).
(28) $R_1 = [\Sigma||F_o| - |F_c||/\Sigma|F_o|] \times 100\%$ and $R_2 = [\Sigma w||F_o| - |F_c||^2/\Sigma w|F_o|^2] \times 100\%$.
(29) Tables 5–12 will appear following these pages in the microfilm edition of this volume of the jorunal.